

Properties of Superfluid Turbulence in a Large Channel

D. D. Awschalom, F. P. Milliken, and K. W. Schwarz
IBM T. J. Watson Research Center, Yorktown Heights, New York 10598
 (Received 28 June 1984)

Pulsed-ion techniques are used in a 1-cm \times 2.3-cm channel to obtain the first spatially resolved measurements of the vortex-line length-density distribution and the normal-fluid velocity field in turbulent counterflow. Also, an upper limit to the structural anisotropy of the vortex tangle is obtained which contradicts earlier claims.

PACS numbers: 67.40.Vs, 67.40.Yv

One of the distinguishing features of superfluid ^4He is that flow through a channel can occur totally without dissipation. Characteristically, such dissipationless flow will exist up to some critical velocity, above which the fluid enters a new flow state wherein it is permeated by a dense, dynamically self-sustaining tangle of quantized vortex lines.^{1,2} This phenomenon is analogous to the transition of a classical fluid to turbulent flow, and the new state is referred to as superfluid turbulence.

The intensity of superfluid turbulence is measured by L , the length of vortex line per unit volume. Measurements of this quantity have revealed a rather complicated onset regime.³ However, at higher driving velocities, where the characteristic interline spacing $\delta \sim L^{-1/2}$ becomes small compared to the channel size, the fluid enters a state of fully developed turbulence. In this limit, the line length density obeys the simple rule

$$L^{1/2} \approx \gamma(T) v_{ns}, \quad (1)$$

where $v_{ns} = |\vec{v}_n - \vec{v}_s|$ is the relative velocity between the normal fluid and the superfluid, which drives the turbulence, and $\gamma(T)$ is a universal function of temperature. The typical behavior seen in various experiments, using quite different techniques to measure L , is shown in Figs. 1(a) and 1(b). The properties of this fully developed state, including a quantitative prediction for $\gamma(T)$, have recently been derived from a first-principles treatment of the dynamics of a homogeneous vortex tangle,⁴ and the theoretical predictions are also shown in Fig. 1. Data from many other experiments could be added to Fig. 1 without changing the picture a great deal.³ Given the very wide variety of channel geometries and experimental techniques that have been used in these studies, the difficulty of obtaining absolute values for L , and the complicated nature of the theoretical problem, the consensus illustrated in Fig. 1 is quite satisfactory.⁹

Apart from the zeroth-order behavior discussed above, very little quantitative information about the properties of fully developed turbulence is available. One obvious point which arises immediately is that L is not necessarily expected to be uniform. Aside from the fact that end effects might be important in the larger channels, there is the question of how the L profile arranges itself across the channel. Thus the possibility of substantial macroscopic inhomogeneities has often been mentioned in the literature. Information on this question, however, is limited to a few experiments^{6,10,11} looking for end effects in large channels, none of which see any significant variations in L along the flow direction. A second important goal is to measure some properties of the vortex tangle other than L . The most fundamental of these has been stressed by Ashton

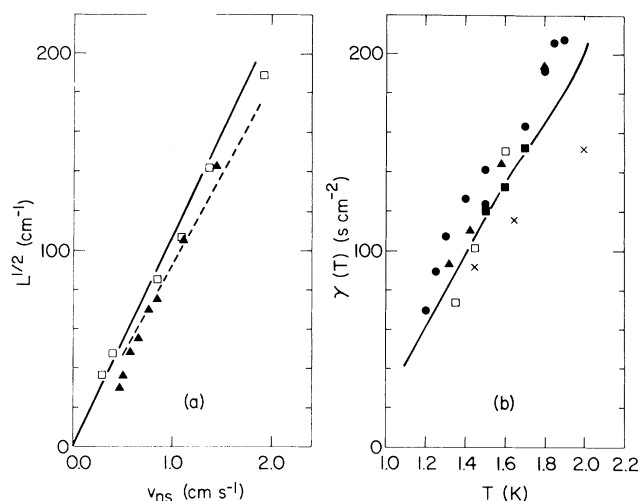


FIG. 1. (a) $L(v_{ns})$ as measured in several large channels near 1.45 K. Triangles, Ref. 5; dashed line, Ref. 6; open squares, our results. (b) $\gamma(T)$ from various channel experiments. Triangles, Ref. 5; crosses, Ref. 6; open squares, our values; squares, Ref. 7; circles, Ref. 8. The solid lines are the theoretical prediction of Ref. 4.

and Northby,¹² who point out that since the vortex tangle is being driven anisotropically by $\bar{v}_n - \bar{v}_s$, its structure can be expected to be anisotropic. As a symptom of this structural anisotropy the vortex tangle should exhibit a net drift rate $\langle \dot{s} \rangle$ (with respect to the superfluid rest frame) in the direction of $\bar{v}_n - \bar{v}_s$. Their experiment finds an easily observed drift rate, which implies a substantial structural anisotropy factor $\langle \dot{s} \rangle / v_{ns}$ for the vortex tangle. Preliminary calculations¹³ along the same lines as those of Ref. 4 predict a relatively small value for this parameter.

In order to learn more about these intriguing questions, we have devised an experiment which yields an accurate determination of both the line-length-density profile and the normal-fluid velocity profile across the channel, and in addition permits a measurement of the vortex-tangle drift rate. The profiles, in particular, represent information of a type never before obtained. The experiment is illustrated in Fig. 2. A counterflow¹⁴ field v_{ns} is established in a 1-cm \times 2.3-cm metal channel, 26 cm in length. Built into the channel walls are an ion source and a variety of interchangeable grid and collector assemblies, one of which is shown in the figure. Both the source and collector assembly are screened by 100-lines/in. electroformed grids set flush with the channel walls. In a typical measurement, a narrow pulse of negative ions is gated into the channel and allowed to propagate to a particular position under the action of a large drift field \mathcal{E} . The field is then switched off, allowing the pulse to remain at this position for as long as several seconds. Some of the ions in the pulse are trapped by quantized vortices, at a rate¹⁵ determined by the local value of L ; the rest drift along with the local normal-fluid velocity \bar{v}_n . Later, \mathcal{E} is turned back on and the surviving pulse is measured in real time by means of one or more fast electrometers as it arrives at the collectors. From the amplitude of the

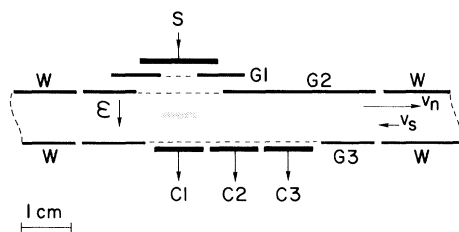


FIG. 2. Experimental geometry. S, tritium source; G1 to G3, pulsed grids with associated guard plates; C1 to C3, collectors at virtual ground; W, grounded channel walls. The dotted region indicates a typical charge pulse, and extends 0.8 cm into the plane of the figure.

observed pulse and where it falls on the collectors, the local values of L and \bar{v}_n can readily be determined as a function of where the pulse was stopped. The spatial resolution achieved with this interrupted-flight technique is better than 1 mm in the present experiment.

In the first series of measurements, C1, C2, and C3 were replaced by a single large collector, and trapping rates were measured in order to determine the L profile across the channel. The results, shown in Fig. 3(a), exhibit a remarkable uniformity of the vortex-line density, its value remaining constant to within our measurement uncertainty of a few percent up to within 1 mm from the walls, where the technique fails. This is true at all power levels studied, and is in marked contrast to the highly inhomogeneous distributions measured when an ultrasonic beam is used to excite the superfluid turbulence.¹⁶ In addition, our measurements show that the velocity dependence of L is accurately given by Eq. (1) [see Fig. 1(a)]. The coefficient $\gamma(T)$ that we observe is shown in Fig. 1(b) and agrees well with the values seen by others.

For the second series of measurements, the pulse was masked so as to have a downstream width of only 1.5 mm. An array of similarly narrow collectors was used to follow the downstream motion of the free ions, and thus to determine the \bar{v}_n profile across the channel as described above. The data, shown in Fig. 3(b), again show no deviation from uniformity, a result which appears surprising in view of the fact that \bar{v}_n must eventually go to zero at the walls. In contrast, if the normal fluid were

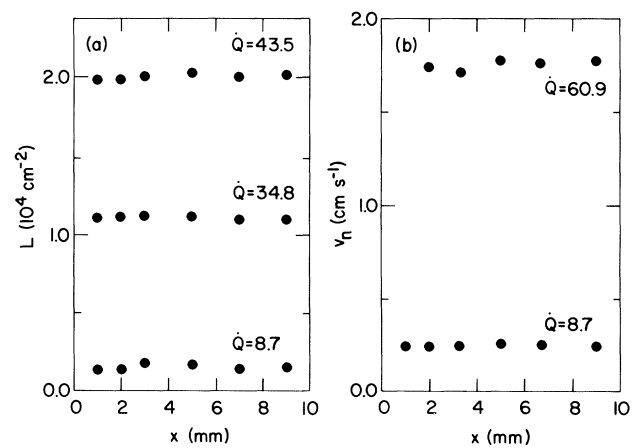


FIG. 3. (a) Line-length-density profiles and (b) normal-fluid velocity profiles as a function of distance across the channel. Heat flux levels are in milliwatts per square centimeter. At $T = 1.45$ K where these data were taken, $v_n = 28.6\dot{Q}$ and $v_{ns} = 31.6\dot{Q}$.

undergoing classical laminar flow, \bar{v}_n would rise from zero at the walls to nearly twice the observed value at the center. The uniformity appears to persist down to quite low values of the driving velocity. Figure 4 compares the value of \bar{v}_n measured at the center of the channel with the mean flow velocity calculated from the heater power. Even at a value of 0.5 mm sec^{-1} , which is close to the expected critical velocity and for which δ is becoming a significant fraction of the channel width, the two agree, thus implying a uniform profile. Evidently, the nonlinear bulk coupling between the vortex tangle and \bar{v}_n is so strong as to self-consistently renormalize both the velocity profile and the line-length distribution to be uniform, the vortex tangle having somewhat the same effect on \bar{v}_n as would a uniform tangle of very fine wire filling the channel. The boundary conditions on \bar{v}_n appear to matter only very near the walls.

A third series of experiments utilizes the geometry of Fig. 2. The drift field is kept large and constant, so that even at the highest \bar{v}_n all untrapped ions reach only C1. The source is turned on for a sufficient time to let the vortex tangle become strongly charged with trapped ions. After the ion source is turned off and the free ions remaining in the channel have been collected, a well-defined signal is observed which arises from the slow rerelease of the trapped charges. If the tangle drifts in the direction of $\bar{v}_n - \bar{v}_s$, the released charge will eventually show up on C2. Although our measure-

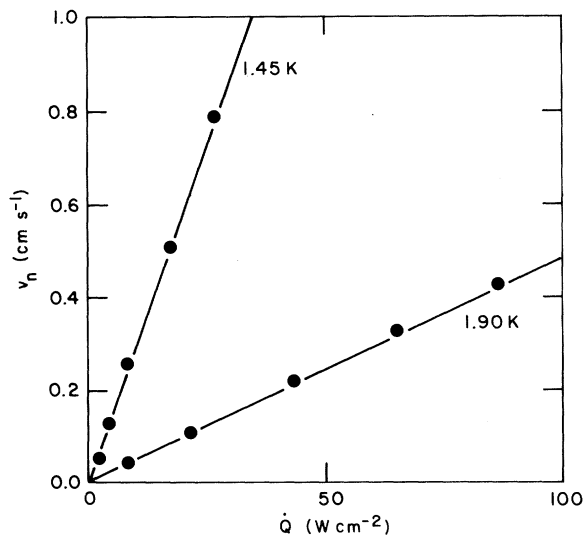


FIG. 4. Normal-fluid velocity at center of channel as a function of the average heat flux density. The lines represent v_n calculated from the independently measured heat input on the assumption that v_n is uniform.

ment is similar to that performed by Ashton and Northby, the results are substantially different. We find that even at our highest driving velocities ($\sim 20 \text{ mm sec}^{-1}$) no rereleased charge whatsoever is observed on C2 or C3, which allows us to conclude that the tangle drift velocity is less than 1 mm sec^{-1} , and yields an upper limit of about 0.2 on the structural anisotropy $\langle \dot{s} \rangle / v_{ns}$ at 1.6 K. This contrasts with values ranging from 0.24 at 1.31 K to 0.42 at 1.59 K reported in Ref. 12. Details aside, we see no evidence of an effect which should be easily observable according to the conclusions of Ref. 12. The present experiment being relatively direct and unambiguous, we infer that any structural anisotropy which may be present is small.

In conclusion, we find that even in our very large channel a fully developed vortex-turbulent state exists with properties which are essentially indistinguishable from those observed in channels several hundred times smaller. The unusually extensive characterization made possible by the interrupted-flight pulsed-ion method shows a state of surprising uniformity both in the turbulence intensity as measured by L , and in the normal-fluid velocity. Interestingly, this situation seems to persist down to the very low turbulence levels characteristic of the onset regime. Furthermore, no indication is found of any substantial structural anisotropy of the kind reported previously. These findings imply that experiments done on channel flow can be interpreted directly in terms of homogeneous-turbulence theory. The historic and plausible objection to this procedure, that there are likely to be substantial inhomogeneities in L , is now ruled out. The strong modification of the normal-fluid velocity field by its interaction with the vortex tangle poses an intriguing theoretical problem which needs to be explored further.

We wish to thank J. T. Tough for pointing out an error in our original manuscript. This research has been supported in part by the National Science Foundation through Grant No. DMR-8005358.

¹R. P. Feynman, in *Progress in Low Temperature Physics*, edited by C. J. Gorter (North-Holland, Amsterdam, 1957), Vol. 1, p. 17.

²W. F. Vinen, Proc. Roy. Soc. London, Ser. A **242**, 493 (1957).

³For a review of this field see J. T. Tough, in *Progress in Low Temperature Physics*, edited by D. F. Brewer (North-Holland, Amsterdam, 1982), Vol. 8, p. 133.

⁴K. W. Schwarz, Phys. Rev. Lett. **49**, 283 (1982).

⁵W. F. Vinen, Proc. Roy. Soc. London, Ser. A **240**, 114 (1957), and **243**, 400 (1957); counterflow in a $0.4 \times 0.78 \times 10\text{-cm}^3$ metal channel.

⁶C. F. Barenghi, K. Park, and R. J. Donnelly, Phys. Lett. **84A**, 435 (1981); C. F. Barenghi, Ph.D. thesis, University of Oregon, 1982 (unpublished); counterflow in a $1.0 \times 1.0 \times 40\text{-cm}^3$ metal channel. The crosses in Fig. 1(b) are revised values from Barenghi's thesis, which differ considerably from the earlier published values.

⁷K. P. Martin and J. T. Tough, Phys. Rev. B **27**, 2788 (1983); counterflow in a $0.10\text{-cm-i.d.} \times 10\text{-cm}$ glass channel.

⁸L. B. Opatowsky and J. T. Tough, Phys. Rev. B **24**, 5420 (1981); pure superflow in a $0.0057 \times 0.057 \times 9.4\text{-cm}^3$ glass channel. According to Ref. 4, γ is expected to exhibit a residual L dependence proportional to $1/\ln(1/L^{1/2}a_0)$. Since the data of Opatowsky and Tough were obtained with $L^{1/2} \sim 10^3$, they have been multiplied by $\ln(10^2a_0)/\ln(10^3a_0) = 0.828$ to compare them with the other data in Fig. 1(b), which were obtained with $L^{1/2} \sim 10^2$.

⁹The theory is not expected to be accurate near the λ

point. All experiments except that of Ref. 6 give values of $\gamma(T)$ which generally exceed the theoretical prediction near T_λ . The explanation for the anomalously low values of $\gamma(T)$ found in Ref. 6 is not yet known.

¹⁰P. E. Dimotakis and J. E. Broadwell, Phys. Fluids **16**, 1787 (1973).

¹¹J. D. Henberger and J. T. Tough, Phys. Rev. B **25**, 3123 (1982).

¹²R. A. Ashton and J. A. Northby, Phys. Rev. Lett. **35**, 1714 (1975); R. A. Ashton, Ph.D. thesis, University of Rhode Island, 1977 (unpublished).

¹³K. W. Schwarz, unpublished.

¹⁴In this mode, a normal-fluid flow is generated by a heater, while the superfluid component flows in the opposite direction to assure zero net mass flow. At our temperatures, $v_n \gg v_s$.

¹⁵The trapping rate is the limit as $\mathcal{E} \rightarrow 0$ of $\frac{2}{3}L\mu\mathcal{E}\sigma$, where μ is the ion mobility and σ is the ion capture diameter measured in rotating-bucket experiments [D. J. Tanner, Phys. Rev. **152**, 121 (1966)].

¹⁶F. P. Milliken, K. W. Schwarz, and C. W. Smith, Phys. Rev. Lett. **48**, 1204 (1982).